arXiv:1411.2954v3 [quant-ph] 27 Jul 2015

Quantum limits to optical point-source localization

MANKEI TSANG[1,2,*]

[1]Department of Electrical and Computer Engineering, National University of Singapore, 4 Engineering Drive 3, Singapore 117583
[2]Department of Physics, National University of Singapore, 2 Science Drive 3, Singapore 117551
[*]mankei@nus.edu.sg

Compiled July 28, 2015

Motivated by the importance of optical microscopes to science and engineering, scientists have pondered for centuries how to improve their resolution and the existence of fundamental resolution limits. In recent years, a new class of microscopes that overcome a long-held belief about the resolution have revolutionized biological imaging. Termed "superresolution" microscopy, these techniques work by accurately locating optical point sources from far field. To investigate the fundamental localization limits, here I derive quantum lower bounds on the error of locating point sources in free space, taking full account of the quantum, nonparaxial, and vectoral nature of photons. These bounds are valid for any measurement technique, as long as it obeys quantum mechanics, and serve as general no-go theorems for the resolution of microscopes. To arrive at analytic results, I focus mainly on the cases of one and two classical monochromatic sources with an initial vacuum optical state. For one source, a lower bound on the root-mean-square position estimation error is on the order of $\lambda_0/\sqrt{N}$, where λ_0 is the free-space wavelength and N is the average number of radiated photons. For two sources, owing to the statistical effect of nuisance parameters, the error bound diverges when their radiated fields overlap significantly. The use of squeezed light to enhance further the accuracy of locating one classical point source and the localization limits for partially coherent sources and single-photon sources are also discussed. The presented theory establishes a rigorous quantum statiscal inference framework for the study of superresolution microscopy and points to the possibility of using quantum techniques for true resolution enhancement.

OCIS codes: *(270.5585) Quantum information and processing; (270.6570) Squeezed states; (100.6640) Superresolution.*

1. INTRODUCTION

The resolution limit of optical microscopes is one of the most important problems in science and engineering. The Abbe-Rayleigh criterion with respect to the free-space wavelength λ_0 has been a widely used resolution limit [1], but it is now well known that the criterion is heuristic in the context of microscopy and superresolution microscopy is possible. An important class of superresolution microscopy, including stimulated-emission-depletion microscopy [2] and photoactivated-localization microscopy [3], relies on the accurate localization of point sources from far field [4]. The localization accuracy, which represents an important measure of the microscope resolution, is then limited by the statistics of the optical measurement [5–8]. Prior analyses of point-source localization accuracy assume classical, scalar, and paraxial optics with statistics specific to the measurement methods [5–8]. On a more fundamental level, however, optics is governed by the quantum theory of electromagnetic field [9], and the existence of more accurate measurement methods [10] and more fundamental quantum limits remains an open question. For example, the superoscillation phenomenon [11] suggests that superresolution diffraction patterns can be obtained in the expense of signal power; can it be exploited to improve the resolution of microscopes [12–14]?

Using a quantum Cramér-Rao bound (QCRB) [15, 16] and the full quantum theory of electromagnetic field [9], here I derive quantum limits to the accuracy of locating point sources. These quantum resolution limits are more general and fundamental than prior classical analyses in the sense that they apply to any measurement method and take full account of the quantum, nonparaxial, and vectoral nature of photons. To arrive at analytic results, I focus mainly on the cases of one and two monochromatic classical sources and an initial vacuum optical state. The possibility of using squeezed light to further enhance the accuracy of locating one point source will also be discussed. To study partially coherent sources, I model incoherence using the concept of nuisance parameters, which are unknown parameters of no primary interest in the context of statistical inference. Quantum bounds for partially coherent sources are then derived by introducing a new generalized QCRB that accounts for nuisance parameters in a special way.

In quantum optics, there has been a substantial literature on quantum imaging; see, for example, Refs. [15, 17–38], but most of them assume certain quantum optical states without considering how they may be generated by objects relevant to mi-

croscopy or consider simply the estimation of mirror displacement. Helstrom's derivation of the QCRB for one point source [15, 17] is the most relevant prior work, although he used the paraxial approximation, did not consider the use of squeezed light, and studied two sources only in the context of binary hypothesis testing [15]. There have also been intriguing claims of superresolution using the nonclassical photon statistics from single-photon sources [34–37], but their protocols have not been analyzed using statistical inference, so even though their images appear sharper, the accuracies of their methods in estimating object parameters remain unclear. To investigate their claims, I also derive a quantum bound for locating a single-photon source.

2. QUANTUM PARAMETER ESTIMATION

Let the initial quantum state of a system be $|\psi\rangle$. After unitary evolution $U(X,T)$ with respect to Hamiltonian $H(X,t)$ as a function of parameters $X=(X_1,X_2,\dots)$, the quantum system is measured with outcome Y. The probability distribution of Y according to Born's rule can be expressed as [15, 16, 39]

$$P(Y|X)=\mathrm{tr}\left[E(Y)U(X,T)|\psi\rangle\langle\psi|U^\dagger(X,T)\right], \tag{1}$$

where $E(Y)$ is the positive operator-valued measure (POVM) that characterizes the quantum measurement and tr denotes the operator trace. Denote the estimator of X using Y as $\tilde{X}(Y)$. The estimation error matrix is defined as

$$\Sigma_{\mu\nu}(X)\equiv\int dY P(Y|X)\left[\tilde{X}_\mu(Y)-X_\mu\right]\left[\tilde{X}_\nu(Y)-X_\nu\right]. \tag{2}$$

For unbiased estimators, the classical Cramér-Rao bound states that [40]

$$\Sigma(X)\geq j^{-1}(X), \tag{3}$$

which means that $\Sigma-j^{-1}$ is positive semidefinite. $j(X)$ is the Fisher information matrix given by

$$j_{\mu\nu}(X)\equiv\int dY P(Y|X)\left[\frac{\partial}{\partial\theta_\mu}\ln P(Y|X)\right]\left[\frac{\partial}{\partial\theta_\nu}\ln P(Y|X)\right]. \tag{4}$$

The bound has been used, for example, in Refs. [7, 8] to evaluate the point-source localization accuracy for a microscope.

It turns out that, for any POVM and thus any measurement in quantum mechanics, another lower bound exists in the form of the QCRB [15, 41]:

$$\Sigma(X)\geq j^{-1}(X)\geq J^{-1}(X), \tag{5}$$

which means that $j^{-1}-J^{-1}$ and $\Sigma-J^{-1}$ are positive-semidefinite. J is the quantum Fisher information (QFI) matrix; it can be obtained by expressing the fidelity $|\langle\psi|U^\dagger(X,T)U(X+\delta X,T)|\psi\rangle|^2$ in the interaction picture [42] and expanding it to the second order of δX [43, 44]. The result is

$$J_{\mu\nu}(X)=4\,\mathrm{Re}\left\langle\Delta g_\mu(X)\Delta g_\nu(X)\right\rangle, \tag{6}$$

where Re denotes the real part, $\langle A\rangle\equiv\langle\psi|A|\psi\rangle$, $\Delta A\equiv A-\langle A\rangle$, and

$$g_\mu(X)\equiv\frac{1}{\hbar}\int_0^T dt U^\dagger(X,t)\frac{\partial H(X,t)}{\partial X_\mu}U(X,t) \tag{7}$$

is the generator of the parameter shift in the Heisenberg picture. For M trials, the QFI is simply multiplied by M, and at least one component of the QCRB can be attained in an asymptotic $M\to\infty$ sense [45]. If one wishes to consider a new set of parameters θ related to the original set X and X can be expressed as a function of θ, the new QFI matrix is simply given by

$$J'_{ab}(\theta)=\sum_{\mu,\nu}\frac{\partial X_\mu}{\partial\theta_a}J_{\mu\nu}(X)\frac{\partial X_\nu}{\partial\theta_b}\bigg|_{X=X(\theta)}. \tag{8}$$

Various generalizations of the QCRB and alternatives are available [15, 46–49], but the presented version suffices to illustrate the pertinent physics. In Sec. 6, the QCRB will be generalized to a Bayesian version that treats nuisance parameters separately and is used to study partially coherent sources.

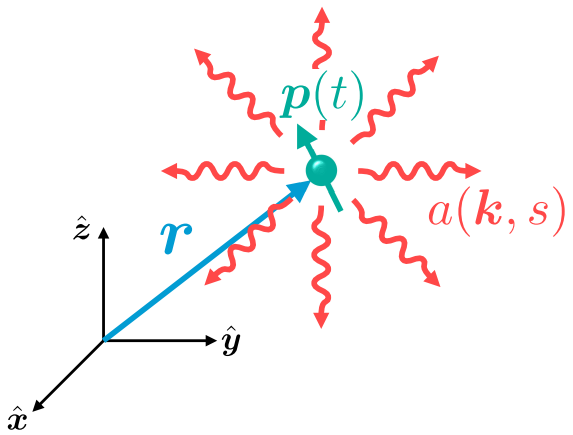

Fig. 1. A classical point source with dipole moment $\boldsymbol{p}(t)$ radiating in free space. Its position $\boldsymbol{r}$ is estimated by measuring the quantum optical field, with $a(\boldsymbol{k},s)$ denoting its annihilation operator.

3. ONE CLASSICAL POINT SOURCE

Consider first a classical point source, as depicted in Fig. 1. The Hamiltonian is [9]

$$H(\boldsymbol{r},t)=H_F+H_I(\boldsymbol{r},t), \tag{9}$$

$$H_F=\sum_s\int d^3k\,\hbar\omega(\boldsymbol{k})a^\dagger(\boldsymbol{k},s)a(\boldsymbol{k},s), \tag{10}$$

$$H_I(\boldsymbol{r},t)=-\boldsymbol{p}(t)\cdot\boldsymbol{E}(\boldsymbol{r}), \tag{11}$$

$$\boldsymbol{E}(\boldsymbol{r})=\sum_s\int d^3k\sqrt{\frac{\hbar\omega}{2(2\pi)^3\epsilon_0}}\left[i\boldsymbol{\varepsilon}(\boldsymbol{k},s)a(\boldsymbol{k},s)e^{i\boldsymbol{k}\cdot\boldsymbol{r}}+\mathrm{H.c.}\right], \tag{12}$$

where $\boldsymbol{k}=k_x\hat{\boldsymbol{x}}+k_y\hat{\boldsymbol{y}}+k_y\hat{\boldsymbol{z}}$ is a wavevector, $(\hat{\boldsymbol{x}},\hat{\boldsymbol{y}},\hat{\boldsymbol{z}})$ denote unit vectors in the Cartesian coordinate system, $\int d^3k\equiv\int_{-\infty}^{\infty}dk_x\int_{-\infty}^{\infty}dk_y\int_{-\infty}^{\infty}dk_z$, s is an index for the two polarizations, $\boldsymbol{\varepsilon}(\boldsymbol{k},s)$ is a unit polarization vector, $\omega(\boldsymbol{k})=c|\boldsymbol{k}|$, c is the speed of light, $\boldsymbol{p}(t)$ is the c-number dipole moment of the source, $\boldsymbol{r}=x\hat{\boldsymbol{x}}+y\hat{\boldsymbol{y}}+z\hat{\boldsymbol{z}}$ is its position, ϵ_0 is the free-space permittivity, $a(\boldsymbol{k},s)$ is an annihilation operator obeying the commutation relation $\left[a(\boldsymbol{k},s),a^\dagger(\boldsymbol{k}',s')\right]=\delta_{ss'}\delta^3(\boldsymbol{k}-\boldsymbol{k}')$, and H.c. denotes the Hermitian conjugate. Since $\boldsymbol{p}(t)$ is a c-number, H_I implements a field displacement operation [9]. The Heisenberg picture of $a(\boldsymbol{k},s)$ is

$$a(\boldsymbol{k},s,t)\equiv U^\dagger(X,t)a(\boldsymbol{k},s)U(X,t) \tag{13}$$

$$=e^{-i\omega t}\left[a(\boldsymbol{k},s)+\alpha(\boldsymbol{k},s,\boldsymbol{r},t)\right], \tag{14}$$

where α is the radiated field. Assuming $\boldsymbol{p}(t) = \boldsymbol{p}_0 e^{-i\omega_0 t} + \text{c.c.}$, where c.c. denotes the complex conjugate, α becomes

$$\alpha(\boldsymbol{k}, s, \boldsymbol{r}, T) = \sqrt{\frac{\omega_0}{2(2\pi)^3 \hbar \epsilon_0}} e^{-i\boldsymbol{k}\cdot\boldsymbol{r}} \boldsymbol{\varepsilon}^*(\boldsymbol{k}, s) \cdot \left[\boldsymbol{p}_0 e^{i(\omega-\omega_0)T/2} \frac{\sin(\omega-\omega_0)T/2}{(\omega-\omega_0)/2} + \boldsymbol{p}_0^* e^{i(\omega+\omega_0)T/2} \frac{\sin(\omega+\omega_0)T/2}{(\omega+\omega_0)/2} \right], \tag{15}$$

which indicates that only the optical modes with $\omega(\boldsymbol{k}) = \omega_0$ grow in time, corresponding to the far field, while all the other near-field modes with $\omega(\boldsymbol{k}) \neq \omega_0$ oscillate. The $\omega(\boldsymbol{k}) = \omega_0$ relation specifies the spatial frequencies available to the far optical fields [50, 51]. Assuming $T \gg 2\pi/\omega_0$, such that $\sin^2[(\omega \pm \omega_0)T/2]/[(\omega \pm \omega_0)/2]^2 \approx 2\pi T \delta(\omega \pm \omega_0)$, using the identity $\sum_s \varepsilon_\mu(\boldsymbol{k}, s)\varepsilon_\nu^*(\boldsymbol{k}, s) = \delta_{\mu\nu} - k_\mu k_\nu / |\boldsymbol{k}|^2$ [9], and switching to the spherical coordinate system for $\boldsymbol{k}$, it can be shown that the average number of radiated photons for an initial vacuum state is

$$N \equiv \sum_s \int d^3k \, |\alpha(\boldsymbol{k}, s, \boldsymbol{r}, T)|^2 \approx \frac{|\boldsymbol{p}_0|^2 \omega_0^3 T}{3\pi\hbar\epsilon_0 c^3}. \tag{16}$$

The far-field limit ($\omega_0 T \to \infty$) will be assumed hereafter.

I now focus on two representative cases: a linearly polarized dipole with $\boldsymbol{p}_0 = p_0 \hat{\boldsymbol{z}}$ and a circularly polarized dipole with $\boldsymbol{p}_0 = p_0(\hat{\boldsymbol{x}} + i\hat{\boldsymbol{y}})/\sqrt{2}$. Taking the unknown parameters to be $\boldsymbol{r}$, the generators for $X = (x, y, z)$ can be expressed, after some algebra, as

$$\Delta g_\mu(\boldsymbol{r}) = -\frac{\sqrt{2}}{W_\mu} \Delta P_\mu(\boldsymbol{r}), \quad \mu \in \{x, y, z\}, \tag{17}$$

$$\Delta P_\mu(\boldsymbol{r}) \equiv \frac{1}{\sqrt{2}i} \left[\Delta b_\mu(\boldsymbol{r}) - \Delta b_\mu^\dagger(\boldsymbol{r}) \right], \tag{18}$$

where Δb_μ is a normalized annihilation operator defined as

$$\Delta b_\mu(\boldsymbol{r}) \equiv W_\mu \sum_s \int d^3k \, \left[-ik_\mu \alpha^*(\boldsymbol{k}, s, \boldsymbol{r}, T) \right] \Delta a(\boldsymbol{k}, s), \tag{19}$$

such that $[\Delta b_\mu(\boldsymbol{r}), \Delta b_\nu^\dagger(\boldsymbol{r})] = \delta_{\mu\nu}$, and the normalization constants W_μ are

$$W_\mu \equiv \left[\sum_s \int d^3k \, k_\mu^2 \, |\alpha_\mu(\boldsymbol{k}, s, \boldsymbol{r}, T)|^2 \right]^{-1/2}. \tag{20}$$

The d^3k integrals can again be computed with the help of the far-field assumption and spherical coordinates. The results depend on $\boldsymbol{p}_0$; for $\boldsymbol{p}_0 = p_0 \hat{\boldsymbol{z}}$,

$$W_x = W_y = \sqrt{\frac{5}{2}} \frac{\lambda_0}{2\pi\sqrt{N}}, \qquad W_z = \frac{\sqrt{5}\lambda_0}{2\pi\sqrt{N}}, \tag{21}$$

and for $\boldsymbol{p}_0 = p_0(\hat{\boldsymbol{x}} + i\hat{\boldsymbol{y}})/\sqrt{2}$,

$$W_x = W_y = \sqrt{\frac{10}{3}} \frac{\lambda_0}{2\pi\sqrt{N}}, \qquad W_z = \sqrt{\frac{5}{2}} \frac{\lambda_0}{2\pi\sqrt{N}}, \tag{22}$$

but the important point here is that they are all on the order of $\lambda_0/\sqrt{N}$, where $\lambda_0 \equiv 2\pi c/\omega_0$ is the free-space wavelength. The QFI becomes

$$J_{\mu\nu}(\boldsymbol{r}) = \frac{8}{W_\mu^2} \left\langle \Delta P_\mu(\boldsymbol{r}) \Delta P_\nu(\boldsymbol{r}) \right\rangle. \tag{23}$$

For an initial vacuum state (or any coherent state), $\langle \Delta P_\mu(\boldsymbol{r}) \Delta P_\nu(\boldsymbol{r}) \rangle = \delta_{\mu\nu}/2$, and the QCRB is hence

$$J_{\mu\nu}(\boldsymbol{r}) = \frac{4}{W_\mu^2} \delta_{\mu\nu}, \qquad \Sigma_{\mu\mu}(\boldsymbol{r}) \geq \frac{W_\mu^2}{4}, \tag{24}$$

meaning that the quantum resolution limit in terms of the root-mean-square error $\sqrt{\Sigma_{\mu\mu}}$ is on the order of $\lambda_0/\sqrt{N}$. I call this limit the quantum shot-noise limit. Generalization to lossless media is straightforward and results simply in λ_0 being replaced by the wavelength in the medium. Sec. 9 shows that a single-photon source also obeys this limit with repeated trials.

Assuming uncorrelated photons, Refs. [5–7, 25] derived a similar limit in the form of $\sigma/\sqrt{N}$, where σ is the width of the imaging point-spread function. While their limit also scales as $1/\sqrt{N}$, all those analyses assume the paraxial approximation and measurement by a photon-counting camera, whereas the quantum shot-noise limit here is valid for any numerical aperture and any measurement, including common methods such as photon counting, homodyne/heterodyne detection, and digital holography. The limit in Refs. [5–7, 25] also implies that the quantum shot-noise limit is reasonably tight, as the camera measurement with suitable postprocessing can at least follow the quantum-optimal shot-noise scaling. Sec. 4 shows that homodyne measurement with a special local-oscillator field can also approach the quantum limit if the radiation is coherent.

For a concrete numerical example, consider the semiclassical paraxial analysis of conventional single-molecule microscopy by Ober *et al.* [7], who used the classical Cramér-Rao bound and a shot-noise assumption to derive a limit of 2.301 nm on the root-mean-square localization error for a free-space wavelength of 520 nm, a numerical aperture of 1.4, a photon collection efficiency of 0.033, a photon flux of 2×10^6 s^{-1}, an acquisition time of 0.01 s. If the efficiency were 1, their limit would become 0.418 nm. In comparison, if I take the refractive index of the immersion oil to be 1.52, $\lambda_0 = 520$ nm$/1.52 = 342$ nm to be the wavelength in the medium, and the photon number to be $N = 2 \times 10^4$, the quantum shot-noise limit according to Eqs. (21), (22), and (24) is $\lambda_0/(2\pi\sqrt{N}) = 0.385$ nm times a constant factor close to 1.

It remains to be seen whether superoscillation techniques are similarly efficient, but the key point here is that, since the quantum bound is valid for any measurement and conventional methods can already get close to it, no other measurement technique is able to offer any significant advantage in resolution enhancement over the conventional methods.

4. QUANTUM ENHANCEMENT

Even though the source is classical, quantum enhancement is possible if the initial state $|\psi\rangle$ is nonclassical, as I now show. If Δg_μ were independent of the parameter, the accuracy could be enhanced by squeezing and measuring the conjugate quadrature [52]. Although $\Delta g_\mu(\boldsymbol{r})$ depends on the unknown $\boldsymbol{r}$ here, the radiated field can be approximated as $\alpha(\boldsymbol{k}, s, \boldsymbol{r}, T) \approx \alpha(\boldsymbol{k}, s, \boldsymbol{r}_0, T)$, resulting in $\Delta g_\mu(\boldsymbol{r}) \approx \Delta g_\mu(\boldsymbol{r}_0)$, provided that

$$|\boldsymbol{r} - \boldsymbol{r}_0| \ll \lambda_0 \tag{25}$$

with respect to a known reference position $\boldsymbol{r}_0$. The acquisition of such prior information will require a fixed amount of overhead resource, but once it is done, one can squeeze the quadrature

$$\Delta Q_\mu(\boldsymbol{r}_0) \equiv \frac{1}{\sqrt{2}} \left[\Delta b_\mu(\boldsymbol{r}_0) + \Delta b_\mu^\dagger(\boldsymbol{r}_0) \right] \tag{26}$$

in the initial state and perform a homodyne measurement of $\Delta Q_\mu(\boldsymbol{r}_0)$ to estimate $\boldsymbol{r}$ much more accurately. Since $[\Delta Q_\mu(\boldsymbol{r}_0), \Delta Q_\nu(\boldsymbol{r}_0)] = 0$, all three quadratures can be squeezed and measured simultaneously in principle. The estimation error becomes

$$\Sigma_{\mu\mu}(\boldsymbol{r}) \approx \frac{W_\mu^2}{2}\left\langle \Delta Q_\mu^2(\boldsymbol{r}_0)\right\rangle, \tag{27}$$

and the error reduction below the shot-noise limit is determined by the squeezing factor, which is limited by the average photon number N_0 in the initial state (not to be confused with N). Using $\left\langle \Delta Q_\mu^2(\boldsymbol{r}_0)\right\rangle + \left\langle \Delta P_\mu^2(\boldsymbol{r}_0)\right\rangle \le 2N_0 + 1$ and the uncertainty relation $\langle \Delta Q_\mu^2\rangle\langle \Delta P_\mu^2\rangle \ge 1/4$, it can be shown that

$$\left\langle \Delta Q_\mu^2(\boldsymbol{r}_0)\right\rangle \ge \frac{f(N_0)}{2}, \quad \left\langle \Delta P_\mu^2(\boldsymbol{r}_0)\right\rangle \le \frac{1}{2f(N_0)}, \tag{28}$$

$$f(N_0) \equiv (2N_0+1)\left[1 - \sqrt{1-(2N_0+1)^{-2}}\right], \tag{29}$$

where

$$f(0) = 1, \qquad f(N_0) \approx \frac{1}{4N_0} \text{ for } N_0 \gg 1. \tag{30}$$

With a zero-mean minimum-uncertainty state and all initial photons in the $\Delta b_\mu(\boldsymbol{r}_0)$ mode, the estimation error becomes

$$\Sigma_{\mu\mu}(\boldsymbol{r}) \approx \frac{W_\mu^2}{2}\left\langle \Delta Q_\mu^2(\boldsymbol{r}_0)\right\rangle = \frac{W_\mu^2}{4} f(N_0). \tag{31}$$

The enhancement factor $f(N_0)$ is optimal, as the QCRB can be further bounded by

$$\Sigma_{\mu\mu}(\boldsymbol{r}) \ge J_{\mu\mu}^{-1}(\boldsymbol{r}) = \frac{W_\mu^2}{8\langle \Delta P_\mu^2(\boldsymbol{r})\rangle} \ge \frac{W_\mu^2}{4} f(N_0). \tag{32}$$

This means that squeezed light with average photon number N_0 can beat the quantum shot-noise limit to the mean-square error by roughly a factor of N_0.

The optical mode to be squeezed has a profile $ik_\mu\alpha(\boldsymbol{k}, s, \boldsymbol{r}_0, T)$. This means that, in real space, the electric field profile of the mode should be the spatial derivative of the radiated field. This kind of squeezing and measurement has actually been demonstrated experimentally, albeit in the paraxial regime, by Taylor *et al.* in the context of particle tracking [38], where the weak scatterer under a strong pump can be modeled as a classical source, similar to the implementation of field displacement by a beam splitter [53], and the spatial mode profile of the squeezed light and the local oscillator is a spatial derivative of the scattered field. To realize an enhancement in practice, accurate phase locking of the squeezed light and the local oscillator to the radiated field and a high measurement efficiency are crucial. Phase locking cannot be achieved with incoherent point sources such as fluorescent markers, but can be done with dielectric particles via Rayleigh scattering [38] or second-harmonic nanoparticles [54, 55]; the latter are especially promising for biological imaging applications [56].

5. TWO CLASSICAL POINT SOURCES

Next, consider two classical point sources at $\boldsymbol{r}$ and $\boldsymbol{r}'$, as shown in Fig. 2. The Hamiltonian is now

$$H(\boldsymbol{r}, \boldsymbol{r}', t) = H_F + H_I(\boldsymbol{r}, \boldsymbol{r}', t), \tag{33}$$

$$H_I(\boldsymbol{r}, \boldsymbol{r}', t) = -\boldsymbol{p}(t)\cdot\boldsymbol{E}(\boldsymbol{r}) - \boldsymbol{p}'(t)\cdot\boldsymbol{E}(\boldsymbol{r}'). \tag{34}$$

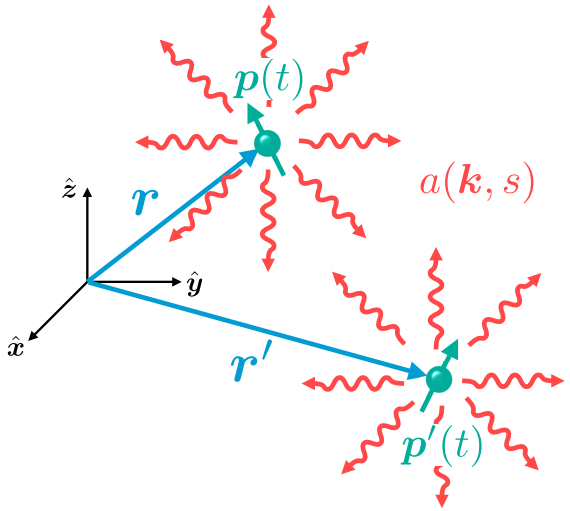

Fig. 2. Two classical point sources with dipole moments $\boldsymbol{p}(t)$ and $\boldsymbol{p}'(t)$ at $\boldsymbol{r}$ and $\boldsymbol{r}'$ with quantum optical radiation.

The Heisenberg picture of $a(\boldsymbol{k}, s)$ becomes $a(\boldsymbol{k}, s, t) = e^{-i\omega t}[a(\boldsymbol{k}, s) + \alpha(\boldsymbol{k}, s, \boldsymbol{r}, t) + \alpha'(\boldsymbol{k}, s, \boldsymbol{r}', t)]$, where α and α' are the radiated fields from the two sources, α is the same as before, and α' has the same expression as α except that $\boldsymbol{p}$ is replaced by $\boldsymbol{p}'$ and $\boldsymbol{r}$ by $\boldsymbol{r}'$. One can then follow the preceding procedure to obtain the QCRB for estimating $\boldsymbol{r}$ and $\boldsymbol{r}'$. To highlight the important physics, however, consider here the estimation of just two parameters $X = (x, x')$. The generators Δg_x and $\Delta g_{x'}$ may not commute, and the QFI matrix for an initial vacuum or any coherent state now has off-diagonal components:

$$J_{xx'}(X) = J_{x'x}(X) = 4\,\mathrm{Re}\sum_s \int d^3k\, k_x^2 \alpha^*(\boldsymbol{k}, s, \boldsymbol{r}, T)\alpha'(\boldsymbol{k}, s, \boldsymbol{r}', T), \tag{35}$$

while J_{xx} remains the same and $J_{x'x'}$ has a similar expression to J_{xx}. J_{xx} and $J_{x'x'}$ still obey a shot-noise scaling with the average photon number, but the nonzero off-diagonal components mean that the parameters act as nuisance parameters to each other, and the QCRB with respect to, say, x is always raised:

$$\Sigma_{xx}(X) \ge \frac{1}{J_{xx}[1-\kappa(X)]}, \tag{36}$$

where the resolution degradation factor, defined as

$$\kappa(X) \equiv \frac{J_{xx'}^2(X)}{J_{xx}J_{x'x'}} = \frac{(\mathrm{Re}\sum_s \int d^3k\, k_x^2 \alpha^*\alpha')^2}{\sum_s \int d^3k\, k_x^2|\alpha|^2 \sum_s \int d^3k\, k_x^2|\alpha'|^2}, \tag{37}$$

is within the range $0 \le \kappa \le 1$ and determined by the overlap between the two differential mode profiles. The nuisance-parameter effect generalizes the Rayleigh criterion and other classical results [8] by revealing a fundamental measurement-independent degradation of resolution for two point sources with overlapping radiation. For example, Fig. 3 plots κ against $|x - x'|/\lambda_0$, assuming $\boldsymbol{p} = \boldsymbol{p}' = \boldsymbol{p}_0 e^{-i\omega_0 t} + \text{c.c.}$, $T \gg 2\pi/\omega_0$, $\boldsymbol{p}_0 = p_0\hat{\boldsymbol{x}}$, $y = y'$, and $z = z'$. $\kappa \approx 0$ for $|x - x'| \gg \lambda_0$, as expected, but it approaches 1 and leads to a diverging QCRB when $|x - x'| \ll \lambda_0$. Sec. 8 shows that the degradation effect should still exist for two partially coherent sources.

The degradation effect can be avoided by minimizing the overlap before each source is located independently. The overlap can be reduced by making the radiated fields separate in

space, time, frequency, quadrature, or polarization; time multiplexing of point sources has especially been the key driver in current superresolution microscopy [2–4].

Note that κ also depends on the relative phase between α and α'. For example, under the assumptions in the caption of Fig. 3, it can be shown that the QFI matrix transformed with respect to the average position $(x + x')/2$ and the separation $x - x'$ is diagonal. The QFI component with respect to the average position still obeys a shot-noise scaling, while the increase in κ can be traced to the increased error in estimating the separation. Similarly, when α and α' are 180° out of phase but otherwise obey the same assumptions, κ remains the same but its increase is now due to the increased error for the average position. An interesting scenario occurs when α and α' are 90° out of phase, the two fields are in orthogonal quadratures, κ becomes zero, and they can be measured separately using homodyne or heterodyne detection. This phenomenon suggests that structured illumination [51, 57–59] can be used to excite the sources, such that their relative phase and amplitude can be controlled to some degree and the overlap can be reduced for certain ranges of parameters.

When the overlap is unavoidable or when the generators do not commute, heterodyne measurements can still be used to measure both quadratures of $a(\boldsymbol{k}, s, T)$ and should have a classical Fisher information within a factor of 1/2 of the QFI. Quantum enhancement may also be possible using entangled squeezed states [60]; the specific experimental design will be left for future studies.

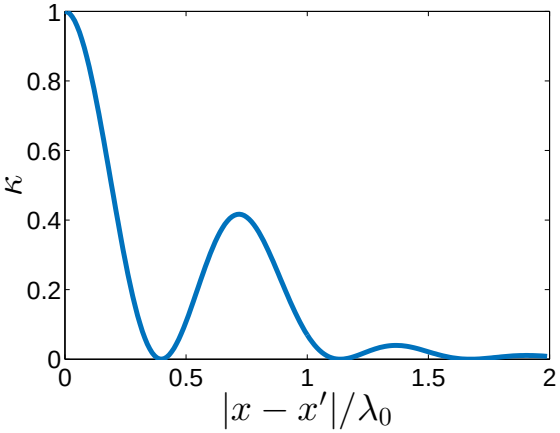

Fig. 3. Plot of the resolution degradation factor κ versus the true separation $|x - x'|/\lambda_0$ between two in-phase point sources, assuming $\boldsymbol{p} = \boldsymbol{p}' = \boldsymbol{p}_0 e^{-i\omega_0 t} + \text{c.c.}$, $T \gg 2\pi/\omega_0$, $\boldsymbol{p}_0 = p_0\hat{\boldsymbol{x}}$, $y = y'$, and $z = z'$. At $|x - x'| = 0$, the Fisher information matrix is singular [61, 62]. κ remains the same for two out-of-phase sources with otherwise the same assumptions.

6. BAYESIAN QUANTUM CRAMÉR-RAO BOUND WITH NUISANCE PARAMETERS

Incoherent sources are characterized by the statistical fluctuations of the fields [9]. For point-source radiation, incoherence originates from the randomness of the amplitude, phase, and direction of the point dipole. In the context of statistical inference, these random variables are most suitably modeled as nuisance parameters. There are many ways to generalize the Cramér-Rao bounds when nuisance parameters are present [63]. The previous sections show one way, which includes the nuisance parameters as part of the wanted parameters X. To derive tighter bounds for other types of nuisance parameters, here I start with a Bayesian QCRB and generalize a classical approach by Miller and Chang [63, 64]. Let Z be a set of nuisance parameters, and suppose first that Z is given. The Bayesian estimation error matrix is

$$\bar{\Sigma}_{\mu\nu}(Z) \equiv \int dX dY P(Y|X,Z) P_{X|Z}(X|Z) \left[\tilde{X}_\mu(Y,Z) - X_\mu\right] \times \left[\tilde{X}_\nu(Y,Z) - X_\nu\right], \tag{38}$$

where $P_{X|Z}(X|Z)$ is the prior distribution of X conditioned on Z. Note that this Bayesian definition of error regards X as a random parameter by averaging over its prior and is different from the frequentist definition in Eq. (2) [40]. A Bayesian quantum Cramér-Rao bound valid for any estimator is given by [46, 47]

$$\bar{\Sigma}(Z) \geq \bar{J}^{-1}(Z), \tag{39}$$

$$\bar{J}(Z) = \mathbb{E}_{X|Z}\left[J(X|Z)\right] + j(Z), \tag{40}$$

where $J(X|Z)$ is the same QFI as before, except that it is now conditioned on Z, $\mathbb{E}_{X|Z}$ denotes expectation over $P_{X|Z}(X|Z)$, and $j(Z)$ is a prior Fisher information defined as

$$j_{\mu\nu}(Z) \equiv \int dX P_{X|Z}(X|Z) \left[\frac{\partial}{\partial X_\mu} \ln P_{X|Z}(X|Z)\right] \times \left[\frac{\partial}{\partial X_\nu} \ln P_{X|Z}(X|Z)\right]. \tag{41}$$

If Z is a random parameter with prior distribution given by $P_Z(Z)$, the estimation error is

$$\Pi_{\mu\nu} \equiv \mathbb{E}_Z\left[\bar{\Sigma}'(Z)\right], \tag{42}$$

$$\bar{\Sigma}'(Z) \equiv \int dX dY P(Y|X,Z) P_{X|Z}(X|Z) \left[\tilde{X}_\mu(Y) - X_\mu\right] \times \left[\tilde{X}_\nu(Y) - X_\nu\right], \tag{43}$$

where $\mathbb{E}_Z$ denotes expectation over P_Z and the estimator $\tilde{X}_\mu(Y)$ can no longer depend on Z. The lower bound in Eq. (39) still holds for $\bar{\Sigma}'(Z)$, so one can obtain a lower bound on Π given by

$$\Pi \geq \mathbb{E}_Z\left[\bar{J}^{-1}(Z)\right]. \tag{44}$$

The important mathematical feature of this bound is that the expectation with respect to the nuisance parameter Z is taken after the inverse of the conditional QFI matrix. This can sometimes lead to a tighter bound than a QCRB that includes Z as part of X. Note also that this Bayesian bound is valid for any estimator, not just the unbiased ones, unlike the claim in Ref. [64]. The tightness of the bound should depend on whether the nuisance parameters can be accurately estimated from the measurements.

7. ONE PARTIALLY COHERENT SOURCE

I now use the new bound to study partially coherent sources. First, consider the example of one point source in Sec. 3, but suppose that the complex dipole amplitude p_0 is unknown. Assuming $Z = p_0$, the quantum state before measurement is

$$\rho = \int d^2 p_0 P_Z(p_0) U(X, p_0, T) \rho_0 U^\dagger(X, p_0, T). \tag{45}$$

If ρ_0 is a vacuum state, $U\rho_0 U^\dagger$ is a coherent state, and ρ is a classical mixed state of light with $P_Z(p_0)$ determining the Sudarshan-Glauber P function [9]. The random p_0 therefore gives rise to a classical partially coherent source model. For an initial vacuum, $\bar{J}(p_0)$ is given by

$$\bar{J}_{\mu\nu}(p_0) = \frac{4}{W_\mu^2(p_0)}\delta_{\mu\nu} + j_{\mu\nu} = \frac{N(p_0)}{C_\mu\lambda_0^2}\delta_{\mu\nu} + j_{\mu\nu}, \tag{46}$$

where W_μ and N now depend on the unknown dipole moment and C_μ is a constant on the order of 1 that can be determined from Eqs. (21) or (22). Assuming that j is diagonal and independent of p_0 and taking the inverse and then the expectation according to Eq. (44), I obtain

$$\Pi_{\mu\mu} \geq \mathbb{E}_{p_0}\left[\frac{1}{4/W_\mu^2(p_0) + j_{\mu\mu}}\right] = \mathbb{E}_{p_0}\left[\frac{1}{N(p_0)/(C_\mu\lambda_0^2) + j_{\mu\mu}}\right]. \tag{47}$$

For example, if $P_Z(p_0)$ corresponds to the P function of a thermal source, the bound can be written in terms of the average radiated photon number $\bar{N}$ as

$$\mathbb{E}_{p_0}\left[\frac{1}{N(p_0)/(C_\mu\lambda_0^2) + j_{\mu\mu}}\right]$$
$$= \frac{C_\mu\lambda_0^2}{\bar{N}}\int_0^\infty dN \exp\left(-\frac{N}{\bar{N}}\right)\frac{1}{N + C_\mu\lambda_0^2 j_{\mu\mu}} \tag{48}$$
$$\approx \frac{C_\mu\lambda_0^2}{\bar{N}}\ln\frac{\bar{N}}{C_\mu\lambda_0^2 j_{\mu\mu}}, \quad \frac{\bar{N}}{C_\mu\lambda_0^2} \gg j_{\mu\mu}. \tag{49}$$

An alternative Bayesian QCRB can be obtained by including p_0 as part of X. In that case, the off-diagonal QFI elements between p_0 and $\boldsymbol{r}$ turn out to be zero, and the expectation with respect to p_0 is taken before the inverse, leading to a bound given by $C_\mu\lambda_0^2/\bar{N}$. The separate treatment of p_0 as nuisance parameter here involves taking the expectation after the inverse, giving rise to an additional factor $\sim \ln\bar{N}$ and thus a tighter bound for large $\bar{N}$. In general, Jensen's inequality can be used to show that the shot-noise scaling with respect to the average photon number $\mathbb{E}_{p_0}[N(p_0)]$ cannot be beat for any nonnegative P function.

8. TWO PARTIALLY COHERENT SOURCES

Next, consider the example of two point sources in Sec. 5, and $Z = (\boldsymbol{p}_0, \boldsymbol{p}_0')$ is now assumed to be unknown to model partially coherent sources. Assuming again that j is diagonal and $X = (x, x')$ is independent of Z,

$$\bar{J}_{xx}(\boldsymbol{p}_0) = \frac{4}{W_x^2(\boldsymbol{p}_0)} + j_{xx}, \tag{50}$$

$$\bar{J}_{x'x'}(\boldsymbol{p}_0') = \frac{4}{W_{x'}^2(\boldsymbol{p}_0')} + j_{x'x'}, \tag{51}$$

$$\bar{J}_{xx'}(\boldsymbol{p}_0, \boldsymbol{p}_0') = \mathbb{E}_X\left[J_{xx'}(\boldsymbol{p}_0, \boldsymbol{p}_0')\right]. \tag{52}$$

$\bar{J}_{xx'}$ is now the expectation of $J_{xx'}$ over $X = (x, x')$, conditioned on the dipole moments. If the two point sources are *a priori* known to be close relative to λ_0, $\bar{J}_{xx'}(\boldsymbol{p}_0, \boldsymbol{p}_0')$ can still have a significant magnitude for certain $(\boldsymbol{p}_0, \boldsymbol{p}_0')$. The bound given by Eq. (44) becomes

$$\Pi_{xx} \geq \mathbb{E}_{(\boldsymbol{p}_0, \boldsymbol{p}_0')}\left\{\frac{1}{\bar{J}_{xx}(\boldsymbol{p}_0)[1 - \bar{\kappa}(\boldsymbol{p}_0, \boldsymbol{p}_0')]}\right\}, \tag{53}$$

where a new resolution degradation factor is defined as

$$\bar{\kappa}(\boldsymbol{p}_0, \boldsymbol{p}_0') \equiv \frac{\bar{J}_{xx'}^2(\boldsymbol{p}_0, \boldsymbol{p}_0')}{\bar{J}_{xx}(\boldsymbol{p}_0)\bar{J}_{x'x'}(\boldsymbol{p}_0')}. \tag{54}$$

The important point here is that $\bar{\kappa}(\boldsymbol{p}_0, \boldsymbol{p}_0')$ can still be close to 1 for certain values of $(\boldsymbol{p}_0, \boldsymbol{p}_0')$ if the two sources are *a priori* known to be close to each other relative to λ_0, $1/[1 - \bar{\kappa}(\boldsymbol{p}_0, \boldsymbol{p}_0')] \gg 1$ is possible, and the expectation over $(\boldsymbol{p}_0, \boldsymbol{p}_0')$ will then be dominated by those large values. In other words, the resolution degradation effect derived for coherent sources must still exist for partially coherent sources if their radiated fields may have significant overlap.

An alternative Bayesian QCRB that includes $(\boldsymbol{p}_0, \boldsymbol{p}_0')$ as part of X can again be computed, but at some stage it involves taking the expectation of $\bar{J}_{xx'}$ with respect to $(\boldsymbol{p}_0, \boldsymbol{p}_0')$ before the inverse is taken. For incoherent sources, this can reduce the off-diagonal components significantly; the resulting bound, while still valid, would be less tight and no longer demonstrate the resolution degradation effect.

9. SINGLE-PHOTON SOURCE

Consider now an initially excited two-level atom in free space. A detailed analysis of atom-photon interaction is formidable [9, 65], but when the initial optical state is vacuum, spontaneous emission can be treated more easily, as the atom must decay to ground state in the long-time limit and the final optical state must contain exactly one photon. Using the continuous Fock space [9], the final optical state in the Schrödinger picture can be written with respect to the vacuum $|0\rangle$ as

$$|\Psi\rangle = c^\dagger|0\rangle, \qquad c^\dagger \equiv \sum_s \int d^3k \phi(\boldsymbol{k}, s) a^\dagger(\boldsymbol{k}, s), \tag{55}$$

where

$$\phi(\boldsymbol{k}, s) = \langle \boldsymbol{k}, s|\Psi\rangle = \langle 0|a(\boldsymbol{k}, s)|\Psi\rangle \tag{56}$$

is the one-photon configuration-space amplitude. Following Chap. III.C of Ref. [65], it can be expressed as

$$\phi(\boldsymbol{k}, s) = \frac{\langle \boldsymbol{k}, s| \otimes \langle g|H_I|e\rangle \otimes |0\rangle}{\hbar[(\omega - \tilde{\omega}_0) + i/(2T_1)]}e^{-i\omega T}, \tag{57}$$

$$H_I = i\omega_0\left(\boldsymbol{\mu}_{12}\sigma - \boldsymbol{\mu}_{12}^*\sigma^\dagger\right)\cdot\boldsymbol{A}(\boldsymbol{r}), \tag{58}$$

$$\boldsymbol{A}(\boldsymbol{r}) = \sum_s \int d^3k \sqrt{\frac{\hbar}{2(2\pi)^3\omega\epsilon_0}}\left[a(\boldsymbol{k}, s)\boldsymbol{\varepsilon}(\boldsymbol{k}, s)e^{i\boldsymbol{k}\cdot\boldsymbol{r}} + \text{h.c.}\right], \tag{59}$$

$$T_1 = \frac{3\pi\hbar\epsilon_0 c^3}{|\boldsymbol{\mu}_{12}|^2\omega_0^3}, \tag{60}$$

where $|e\rangle$ and $|g\rangle$ are the excited and ground atomic states, ω_0 is the atomic resonance frequency, $\tilde{\omega}_0$ is the Lamb-shifted atomic frequency, T_1 is the decay time, $\boldsymbol{\mu}_{12}$ is the off-diagonal atomic dipole moment, and $\sigma \equiv |g\rangle\langle e|$ is the atomic lowering operator. The result is

$$\phi(\boldsymbol{k}, s) = \frac{1}{i(\omega - \tilde{\omega}_0) + 1/(2T_1)}\sqrt{\frac{\omega_0^2}{2(2\pi)^3\hbar\omega\epsilon_0}}\boldsymbol{\mu}_{12}\cdot\boldsymbol{\varepsilon}^*(\boldsymbol{k}, s)$$
$$\times e^{-i\boldsymbol{k}\cdot\boldsymbol{r} - i\omega T}. \tag{61}$$

Consider the fidelity

$$F = \left|\langle 0|c(X)c^\dagger(X+\delta X)|0\rangle\right|^2 \tag{62}$$

$$= \left|\left[c(X), c^\dagger(X+\delta X)\right]\right|^2 \tag{63}$$

$$\approx 1 + \sum_{\mu,\nu}\delta X_\mu \delta X_\nu \left\{ \mathrm{Re}\left[c, \frac{\partial^2 c^\dagger}{\partial X_\mu \partial X_\nu}\right] + \mathrm{Im}\left[c, \frac{\partial c^\dagger}{\partial X_\mu}\right] \mathrm{Im}\left[c, \frac{\partial c^\dagger}{\partial X_\nu}\right] \right\}, \tag{64}$$

where the fact

$$\mathrm{Re}\langle 0|c\frac{\partial c^\dagger}{\partial X_\mu}|0\rangle = \mathrm{Re}\left[c, \frac{\partial c^\dagger}{\partial X_\mu}\right] = 0 \tag{65}$$

due to $\langle 0|c(X+\delta X)c^\dagger(X+\delta X)|0\rangle = \langle 0|c(X)c^\dagger(X)|0\rangle = 1$ has been used. It can further be shown that

$$\left[c, \frac{\partial c^\dagger}{\partial X_\mu}\right] = \sum_s \int d^3k \phi^*(\boldsymbol{k}, s)\frac{\partial \phi(\boldsymbol{k}, s)}{\partial X_\mu} = 0, \tag{66}$$

leading to a QFI given by

$$J_{\mu\nu} = -4\,\mathrm{Re}\left[c, \frac{\partial^2 c^\dagger}{\partial X_\mu \partial X_\nu}\right] \tag{67}$$

$$= -4\,\mathrm{Re}\sum_s \int d^3k \phi^*(\boldsymbol{k}, s)\frac{\partial^2 \phi(\boldsymbol{k}, s)}{\partial X_\mu \partial X_\nu}. \tag{68}$$

$$= 4\,\mathrm{Re}\sum_s \int d^3k \frac{k_\mu k_\nu}{(\omega - \tilde{\omega}_0)^2 + 1/(4T_1^2)} \frac{\omega_0^2}{2(2\pi)^3 \hbar \omega \epsilon_0} \times |\boldsymbol{\mu}_{12}\cdot\boldsymbol{\varepsilon}^*(\boldsymbol{k}, s)|^2. \tag{69}$$

Assuming that the decay time is much longer than the optical period ($T_1 \gg 2\pi/\tilde{\omega}_0$) and the Lamb shift is much smaller than the optical ω_0 ($\tilde{\omega}_0 \approx \omega_0$), the QFI becomes

$$J_{\mu\nu} \approx 4\,\mathrm{Re}\sum_s \int d^3k k_\mu k_\nu 2\pi T_1 \delta(\omega - \omega_0)\frac{\omega_0^2}{2(2\pi)^3 \hbar \omega \epsilon_0} \times |\boldsymbol{\mu}_{12}\cdot\boldsymbol{\varepsilon}^*(\boldsymbol{k}, s)|^2. \tag{70}$$

This turns out to be identical to the QFI derived in Sec. 3 for an $N = 1$ classical source:

$$J_{\mu\nu} = \frac{4\delta_{\mu\nu}}{NW_\mu^2} \sim \frac{\delta_{\mu\nu}}{\lambda_0^2}, \qquad \Sigma_{\mu\mu} \geq J_{\mu\mu}^{-1} = \frac{NW_\mu^2}{4} \sim \lambda_0^2, \tag{71}$$

where N is defined in Eq. (16) and W_μ is defined in Eq. (20) and given by Eqs. (21) or Eqs. (22), such that NW_μ^2 is on the order of λ_0^2. This result shows that a single-photon source offers no fundamental advantage over a classical source that emits one photon on average. Superresolution beyond the classical Abbe-Rayleigh limit can still be obtained, however, if the experiment can be repeated. The QFI is then multiplied by the number of trials M, which is also the total number of emitted photons, and the resulting QCRB is identical to that for a classical source with M replacing N. The experiments reported by Refs. [35–37] certainly involved a large number of measurements of many photons in total, which can explain the apparent superresolution, but it remains to be seen whether their methods are accurate or efficient in estimating object parameters.

For two atoms with large separation ($|\boldsymbol{r} - \boldsymbol{r}'| \gg \lambda_0$), the one-atom analysis is expected to be applicable to each atom independently. The analysis of two close atoms is much more challenging because of atomic cooperative effects such as the Dicke superradiance [9] and the Förster resonance energy transfer [4]. Beyond the current assumption of spontaneous emission, it will also be interesting, though highly nontrivial, to analyze the interaction between two-level atoms and other states of light, such as coherent states or squeezed states, and investigate their quantum localization limits and the possibility of quantum enhancement.

10. CONCLUSION

I have derived quantum limits to point-source localization using quantum estimation theory and the quantum theory of electromagnetic fields. These results not only provide general no-go theorems concerning the microscope resolution, they should also motivate further progress in microscopy through classical or quantum techniques beyond the current assumptions. For example, the presented theory may be applied to other more exotic quantum states of light interacting with quantum sources, such as multilevel atoms [9, 66], quantum dots [35, 67], diamond defects [36, 37, 68], and second-harmonic nanoparticles [54–56]. It is also possible to generalize the current formalism for open quantum systems [69–72] to account for mixed states, decoherence, optical losses, background noises, and imperfect measurement efficiency. The phenomenon of fluorescence intermittency or blinking represents another interesting challenge to the statistical analysis, as a fluorescent source can turn itself on and off randomly and the localization of two blinking sources offers another route to superresolution [73]. If done with care, the application of quantum information science to microscopy is destined to yield sound insights and opportunities in both fields.

FUNDING INFORMATION

Singapore National Research Foundation (NRF-NRFF2011-07).

REFERENCES

1. M. Born and E. Wolf, *Principles of Optics: Electromagnetic Theory of Propagation, Interference and Diffraction of Light* (Cambridge University Press, Cambridge, 1999).
2. S. W. Hell, "Far-field optical nanoscopy," Science **316**, 1153–1158 (2007).
3. E. Betzig, G. H. Patterson, R. Sougrat, O. W. Lindwasser, S. Olenych, J. S. Bonifacino, M. W. Davidson, J. Lippincott-Schwartz, and H. F. Hess, "Imaging intracellular fluorescent proteins at nanometer resolution," Science **313**, 1642–1645 (2006).
4. W. E. Moerner, "New directions in single-molecule imaging and analysis," Proceedings of the National Academy of Sciences **104**, 12596–12602 (2007).
5. N. Bobroff, "Position measurement with a resolution and noise-limited instrument," Review of Scientific Instruments **57**, 1152–1157 (1986).
6. R. E. Thompson, D. R. Larson, and W. W. Webb, "Precise nanometer localization analysis for individual fluorescent probes," Biophysical Journal **82**, 2775–2783 (2002).
7. R. J. Ober, S. Ram, and E. S. Ward, "Localization accuracy in single-molecule microscopy," Biophysical Journal **86**, 1185–1200 (2004).
8. S. Ram, E. S. Ward, and R. J. Ober, "Beyond rayleigh's criterion: A resolution measure with application to single-molecule microscopy," Proceedings of the National

Academy of Sciences of the United States of America **103**, 4457–4462 (2006).
9. L. Mandel and E. Wolf, *Optical Coherence and Quantum Optics* (Cambridge University Press, Cambridge, 1995).
10. C. J. R. Sheppard, "The optics of microscopy," Journal of Optics A: Pure and Applied Optics **9**, S1 (2007).
11. M. V. Berry and S. Popescu, "Evolution of quantum superoscillations and optical superresolution without evanescent waves," Journal of Physics A: Mathematical and General **39**, 6965 (2006).
12. N. I. Zheludev, "What diffraction limit?" Nature Materials **7**, 420–422 (2008).
13. F. M. Huang and N. I. Zheludev, "Super-resolution without evanescent waves," Nano Letters **9**, 1249–1254 (2009).
14. H. J. Hyvärinen, S. Rehman, J. Tervo, J. Turunen, and C. J. R. Sheppard, "Limitations of superoscillation filters in microscopy applications," Opt. Lett. **37**, 903–905 (2012).
15. C. W. Helstrom, *Quantum Detection and Estimation Theory* (Academic Press, New York, 1976).
16. A. S. Holevo, *Statistical Structure of Quantum Theory* (Springer-Verlag, Berlin, 2001).
17. C. W. Helstrom, "Estimation of object parameters by a quantum-limited optical system," J. Opt. Soc. Am. **60**, 233–239 (1970).
18. M. I. Kolobov, "The spatial behavior of nonclassical light," Rev. Mod. Phys. **71**, 1539–1589 (1999).
19. C. Fabre, J. B. Fouet, and A. Maître, "Quantum limits in the measurement of very small displacements in optical images," Optics Letters **25**, 76–78 (2000).
20. N. Treps, N. Grosse, W. P. Bowen, C. Fabre, H.-A. Bachor, and P. K. Lam, "A quantum laser pointer," Science **301**, 940–943 (2003).
21. S. Barnett, C. Fabre, and A. Maıtre, "Ultimate quantum limits for resolution of beam displacements," The European Physical Journal D - Atomic, Molecular, Optical and Plasma Physics **22**, 513–519 (2003).
22. A. N. Boto, P. Kok, D. S. Abrams, S. L. Braunstein, C. P. Williams, and J. P. Dowling, "Quantum interferometric optical lithography: Exploiting entanglement to beat the diffraction limit," Phys. Rev. Lett. **85**, 2733–2736 (2000).
23. H. Li, V. A. Sautenkov, M. M. Kash, A. V. Sokolov, G. R. Welch, Y. V. Rostovtsev, M. S. Zubairy, and M. O. Scully, "Optical imaging beyond the diffraction limit via dark states," Phys. Rev. A **78**, 013803 (2008).
24. R. W. Boyd and J. P. Dowling, "Quantum lithography: status of the field," Quantum Information Processing **11**, 891–901 (2012).
25. M. Tsang, "Quantum imaging beyond the diffraction limit by optical centroid measurements," Phys. Rev. Lett. **102**, 253601 (2009).
26. H. Shin, K. W. C. Chan, H. J. Chang, and R. W. Boyd, "Quantum spatial superresolution by optical centroid measurements," Phys. Rev. Lett. **107**, 083603 (2011).
27. L. A. Rozema, J. D. Bateman, D. H. Mahler, R. Okamoto, A. Feizpour, A. Hayat, and A. M. Steinberg, "Scalable spatial superresolution using entangled photons," Phys. Rev. Lett. **112**, 223602 (2014).
28. V. Giovannetti, S. Lloyd, L. Maccone, and J. H. Shapiro, "Sub-rayleigh-diffraction-bound quantum imaging," Phys. Rev. A **79**, 013827 (2009).
29. R. Nair and B. J. Yen, "Optimal quantum states for image sensing in loss," Phys. Rev. Lett. **107**, 193602 (2011).
30. S. Pirandola, "Quantum reading of a classical digital memory," Phys. Rev. Lett. **106**, 090504 (2011).
31. C. A. Pérez-Delgado, M. E. Pearce, and P. Kok, "Fundamental limits of classical and quantum imaging," Phys. Rev. Lett. **109**, 123601 (2012).
32. P. R. Hemmer and T. Zapata, "The universal scaling laws that determine the achievable resolution in different schemes for super-resolution imaging," Journal of Optics **14**, 083002 (2012).
33. P. C. Humphreys, M. Barbieri, A. Datta, and I. A. Walmsley, "Quantum enhanced multiple phase estimation," Phys. Rev. Lett. **111**, 070403 (2013).
34. O. Schwartz and D. Oron, "Improved resolution in fluorescence microscopy using quantum correlations," Phys. Rev. A **85**, 033812 (2012).
35. O. Schwartz, J. M. Levitt, R. Tenne, S. Itzhakov, Z. Deutsch, and D. Oron, "Superresolution microscopy with quantum emitters," Nano Letters **13**, 5832–5836 (2013).
36. J.-M. Cui, F.-W. Sun, X.-D. Chen, Z.-J. Gong, and G.-C. Guo, "Quantum statistical imaging of particles without restriction of the diffraction limit," Phys. Rev. Lett. **110**, 153901 (2013).
37. D. Gatto Monticone, K. Katamadze, P. Traina, E. Moreva, J. Forneris, I. Ruo-Berchera, P. Olivero, I. P. Degiovanni, G. Brida, and M. Genovese, "Beating the abbe diffraction limit in confocal microscopy via nonclassical photon statistics," Phys. Rev. Lett. **113**, 143602 (2014).
38. M. A. Taylor, J. Janousek, V. Daria, J. Knittel, B. Hage, H.-A. Bachor, and W. P. Bowen, "Biological measurement beyond the quantum limit," Nature Photonics **7**, 229–233 (2013).
39. H. M. Wiseman and G. J. Milburn, *Quantum Measurement and Control* (Cambridge University Press, Cambridge, 2010).
40. H. L. Van Trees, *Detection, Estimation, and Modulation Theory, Part I.* (John Wiley & Sons, New York, 2001).
41. S. L. Braunstein and C. M. Caves, "Statistical distance and the geometry of quantum states," Phys. Rev. Lett. **72**, 3439–3443 (1994).
42. M. Tsang and R. Nair, "Fundamental quantum limits to waveform detection," Phys. Rev. A **86**, 042115 (2012).
43. M. G. A. Paris, "Quantum estimation for quantum technology," International Journal of Quantum Information **7**, 125–137 (2009).
44. A. De Pasquale, D. Rossini, P. Facchi, and V. Giovannetti, "Quantum parameter estimation affected by unitary disturbance," Phys. Rev. A **88**, 052117 (2013).
45. A. Fujiwara, "Strong consistency and asymptotic efficiency for adaptive quantum estimation problems," Journal of Physics A: Mathematical and General **39**, 12489 (2006).
46. H. P. Yuen and M. Lax, "Multiple-parameter quantum estimation and measurement of nonselfadjoint observables," IEEE Transactions on Information Theory **19**, 740–750 (1973).
47. M. Tsang, H. M. Wiseman, and C. M. Caves, "Fundamental quantum limit to waveform estimation," Phys. Rev. Lett. **106**, 090401 (2011).
48. M. Tsang, "Ziv-Zakai error bounds for quantum parameter estimation," Phys. Rev. Lett. **108**, 230401 (2012).
49. D. W. Berry, M. Tsang, M. J. W. Hall, and H. M. Wiseman, "The quantum Bell-Ziv-Zakai bounds and Heisenberg limits for waveform estimation," ArXiv e-prints (2014).
50. J. W. Goodman, *Introduction to Fourier Optics* (McGraw-Hill, New York, 2004).
51. R. Heintzmann and M. G. L. Gustafsson, "Subdiffraction

resolution in continuous samples," Nature Photonics **3**, 362–364 (2009).
52. S. L. Braunstein, C. M. Caves, and G. J. Milburn, "Generalized uncertainty relations: Theory, examples, and lorentz invariance," Annals of Physics **247**, 135 – 173 (1996).
53. M. G. Paris, "Displacement operator by beam splitter," Physics Letters A **217**, 78 – 80 (1996).
54. Y. Pu, M. Centurion, and D. Psaltis, "Harmonic holography: a new holographic principle," Appl. Opt. **47**, A103–A110 (2008).
55. C.-L. Hsieh, R. Grange, Y. Pu, and D. Psaltis, "Three-dimensional harmonic holographic microcopy using nanoparticles as probes for cell imaging," Opt. Express **17**, 2880–2891 (2009).
56. W. P. Dempsey, S. E. Fraser, and P. Pantazis, "Shg nanoprobes: Advancing harmonic imaging in biology," BioEssays **34**, 351–360 (2012).
57. M. G. L. Gustafsson, D. A. Agard, and J. W. Sedat, "I5m: 3d widefield light microscopy with better than 100 nm axial resolution," Journal of Microscopy **195**, 10–16 (1999).
58. M. G. L. Gustafsson, "Surpassing the lateral resolution limit by a factor of two using structured illumination microscopy," Journal of Microscopy **198**, 82–87 (2000).
59. R. Heintzmann and C. G. Cremer, "Laterally modulated excitation microscopy: improvement of resolution by using a diffraction grating," Proc. SPIE **3568**, 185–196 (1999).
60. M. G. Genoni, M. G. A. Paris, G. Adesso, H. Nha, P. L. Knight, and M. S. Kim, "Optimal estimation of joint parameters in phase space," Phys. Rev. A **87**, 012107 (2013).
61. P. Stoica and T. L. Marzetta, "Parameter estimation problems with singular information matrices," Signal Processing, IEEE Transactions on **49**, 87–90 (2001).
62. A. Rotnitzky, D. R. Cox, M. Bottai, and J. Robins, "Likelihood-based inference with singular information matrix," Bernoulli **6**, 243–284 (2000).
63. H. L. Van Trees and K. L. Bell, eds., *Bayesian Bounds for Parameter Estimation and Nonlinear Filtering/Tracking* (Wiley-IEEE, Piscataway, 2007).
64. R. W. Miller and C. B. Chang, "A modified cramér-rao bound and its applications (corresp.)," IEEE Transactions on Information Theory **24**, 398–400 (1978).
65. C. Cohen-Tannoudji, J. Dupont-Roc, and G. Grynberg, *Atom-Photon Interactions* (Wiley-VCH Verlag GmbH, Weinheim, 2004).
66. M. O. Scully and M. S. Zubairy, *Quantum Optics* (Cambridge University Press, Cambridge, 1997).
67. X. Michalet, F. F. Pinaud, L. A. Bentolila, J. M. Tsay, S. Doose, J. J. Li, G. Sundaresan, A. M. Wu, S. S. Gambhir, and S. Weiss, "Quantum dots for live cells, in vivo imaging, and diagnostics," Science **307**, 538–544 (2005).
68. L. T. Hall, G. C. G. Beart, E. A. Thomas, D. A. Simpson, L. P. McGuinness, J. H. Cole, J. H. Manton, R. E. Scholten, F. Jelezko, J. Wrachtrup, S. Petrou, and L. C. L. Hollenberg, "High spatial and temporal resolution wide-field imaging of neuron activity using quantum nv-diamond," Sci. Rep. **2**, 401 (2012).
69. B. M. Escher, R. L. de Matos Filho, and L. Davidovich, "General framework for estimating the ultimate precision limit in noisy quantum-enhanced metrology," Nature Physics **7**, 406–411 (2011).
70. R. Demkowicz-Dobrzański, J. Kołodyński, and M. Guţă, "The elusive Heisenberg limit in quantum-enhanced metrology," Nature Communications **3**, 1063 (2012).
71. M. Tsang, "Quantum metrology with open dynamical systems," New Journal of Physics **15**, 073005 (2013).
72. S. I. Knysh, E. H. Chen, and G. A. Durkin, "True Limits to Precision via Unique Quantum Probe," ArXiv e-prints (2014).
73. K. Lidke, B. Rieger, T. Jovin, and R. Heintzmann, "Superresolution by localization of quantum dots using blinking statistics," Opt. Express **13**, 7052–7062 (2005).